Applied Surface Science 361 (2016) 49–56

Contents lists available at ScienceDirect

Applied Surface Science

journal homepage: www.elsevier.com/locate/apsusc

Preparation and tribological behavior of Ni-graphene composite coating under room temperature

Juanjuan Chen [a], Jianliang Li [a,b,*], Dangsheng Xiong [a,b], Yong He [a], Yujuan Ji [a], Yongkun Qin [a]

[a] School of Material Science and Engineering, Nanjing University of Science and Technology, Nanjing 210094, China
[b] Jiangsu Key Laboratory of Advanced Micro and Nano Materials, Nanjing University of Science and Technology, Nanjing 210094, China

ARTICLE INFO

Article history:
Received 22 July 2015
Received in revised form 9 November 2015
Accepted 9 November 2015
Available online 14 November 2015

Keywords:
Composite coating
Friction and wear
Tribological behavior

ABSTRACT

In this paper, Ni-graphene composite coatings with different graphene addition amounts were prepared on 45 steel disk by using dipulse composite electrodeposition technology. Meanwhile, the influence of plating time, bath temperature and load on friction and wear of the coating was studied. The tribological behavior of composite coating was tested against a Si_3N_4 ceramic ball under dry condition. Cross-sectional morphologies showed that Ni-graphene coating was successfully coated on the substrate with an average thickness of 85 ± 5 μm. XRD analysis concluded that with the increase of addition amount of graphene, the average crystallite size of coating decreased. EDS analyses and Raman spectra proved the presence of graphene. Friction coefficient of composite coating decreased with the increase of graphene addition amounts, while the hardness increased. Meanwhile, the wear resistance of composite coating improved. The optimum experimental conditions were obtained.

1. Introduction

Metal matrix composite coatings containing nano-sized particles of reinforcing phase can be effectively deposited by electrodeposition to enhance the corrosion and wear performance of materials [1]. The problem of stable suspension of nanoparticles in the plating solution is usually overcome by addition of suitable surfactant. The particles reach the surface of the substrate by stirring and get deposited on the substrate metal resulting in composite coating having thickness from tens to hundreds of micrometers. It has already been reported that inclusion of nanoparticles in composite coatings enhances the hardness, corrosion resistance, lubrication and antifriction properties of steel [2]. Also, these properties are reported to be dependent on the experimental parameters like current density, pH, bath constituent's concentrations and the nature of particle [3]. Amongst many metal-based composite coatings, Ni matrix composite coatings are of great importance because of their high hardness and wear resistance.

He et al. [4] prepared Ni-diamond composite coatings containing 1.47–15.6 wt% diamond particle by composite electrodeposition. They reported that Ni-diamond composite coating had a completely different structure from pure nickel coating and the presence of diamond particles provided better corrosion resistance than pure nickel coating. Carpenter et al. [5] prepared nickel-carbon nanotube (Ni-CNT) composite coatings having different CNT volume fractions by electrodeposition and examined their friction and wear properties under dry sliding reciprocating motion. The results indicated that Ni-CNT coatings had higher and more consistent hardness as well as improved wear resistance.

Since, the successful preparation of graphene from exfoliation of graphite by Geim and Novoselov in 2004 [6], it has attracted a lot of attention from scientists due to its excellent properties. Because of smaller shear force between its layers, it has lower friction coefficient than graphite in theory, thus we hope it can make contributions to antifriction and lubrication. Kim et al. [7] prepared graphene films on the surface of SiO_2/Si by chemical vapor deposition (CVD), used Cu and Ni as catalyst. Then they evaluated the friction performance by atomic force microscope (AFM), finding that the friction coefficient of Ni-graphene was only 0.03. Venkatesha et al. [8] successfully prepared Ni-graphene composite coatings on mild steel specimens by electrodeposition and analyzed their corrosion behavior. They reported a change in the surface morphology of graphene resulting in fine grained structure with higher

* Corresponding author at: School of Material Science and Engineering, Nanjing University of Science and Technology, Nanjing 210094, China.
E-mail address: jianliangli@163.com (J. Li).

http://dx.doi.org/10.1016/j.apsusc.2015.11.094
0169-4332/

Table 1
Bath composition and operating conditions.

Component	
$NiSO_4{\cdot}6H_2O$	240 g/L
$NiCl_2{\cdot}6H_2O$	45 g/L
H_3BO_3	30 g/L
Na_2SO_4	20 g/L
SDBS	0.05 g
Graphene	0.1 g/L, 0.2 g/L, 0.3 g/L, 0.4 g/L
Temperature	50–80 °C
Time	2 h, 4 h, 6 h, 8 h
Current density	1 A dm^{-2}
Stirring rate	750 rpm

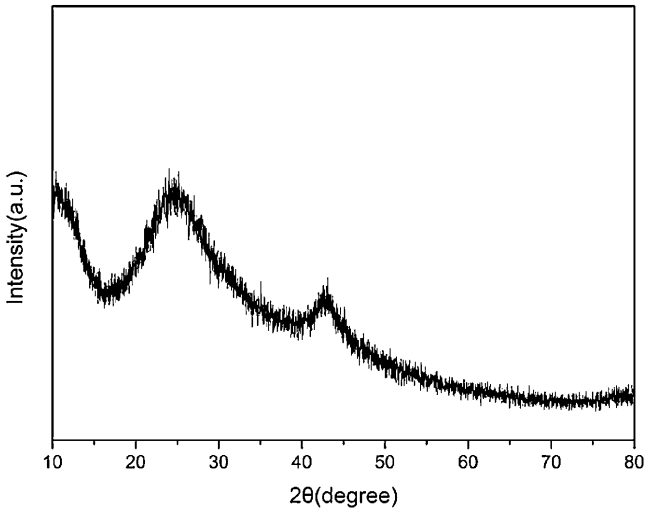

Fig. 1. XRD pattern of graphene.

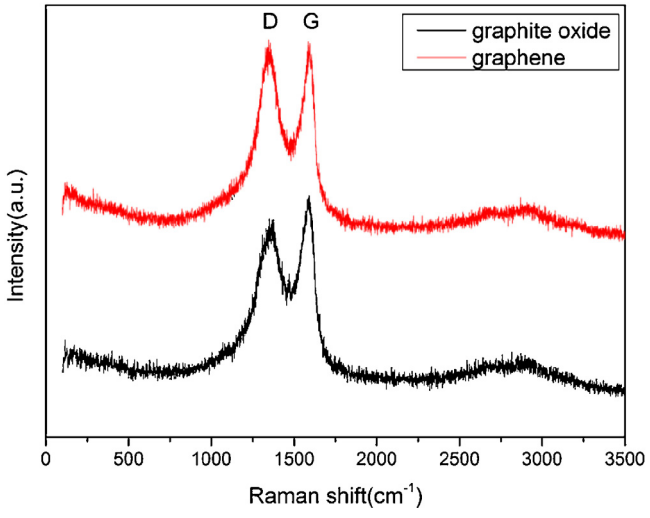

Fig. 2. Raman spectra of graphite oxide and graphene.

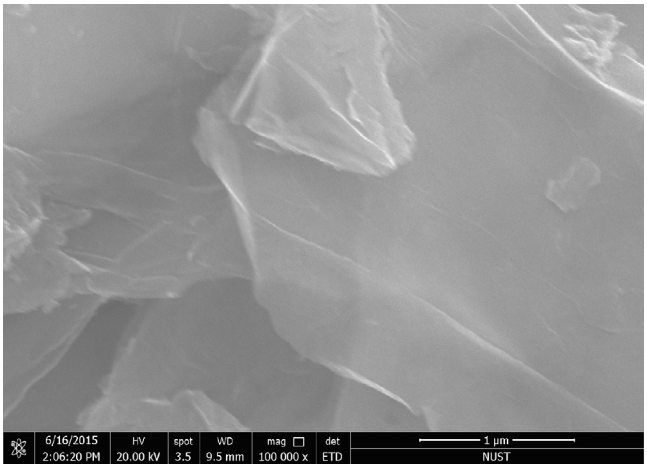

Fig. 3. SEM photomicrographs of graphene.

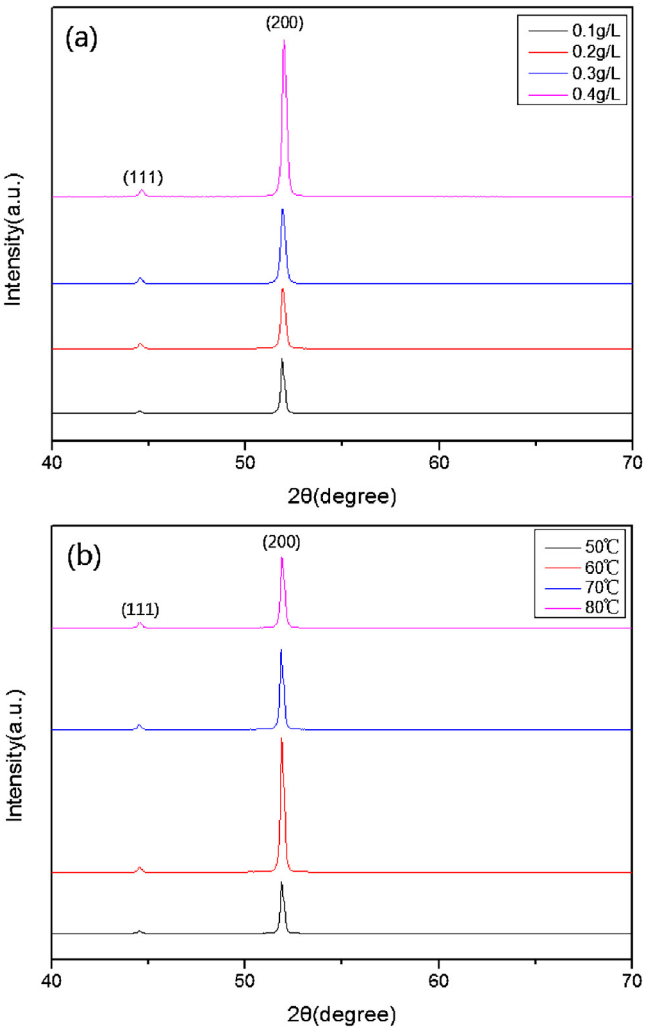

Fig. 4. XRD patterns of composite coatings with different addition amounts of graphene (a) and under different bath temperature with 0.1 g/L graphene (b).

hardness and an improvement in corrosion resistance in comparison to the pure Ni coating.

In the present work, Ni-graphene composite coatings with different additions of graphene have been prepared by electrodeposition and the effect of experimental parameters such as plating time, bath temperature and composition on the mechanical properties of composite coatings has been examined. The friction and wear characteristics of the composite coatings under dry sliding contact have also been determined to understand the influence of graphene on the tribological behavior of Ni graphene coatings.

2. Experimental

2.1. Synthesis of graphene

2.1.1. Synthesis of graphite oxide

Graphite oxide was prepared following a modified Hummers method [9]. To prepare the graphite oxide 1 g graphite powder was dispersed in a solution containing 20 ml concentrated H_2SO_4 (98 wt%) and 5 ml H_3PO_4 (85 wt%) and stirred magnetically for mixing properly. A calculated amount of $KMnO_4$ (6 g) was also added to the above solution slowly, while stirring it continuously. The temperature of mixture was kept below 20 °C in a water bath. After oxidizing for 1 h, the reaction mixture was transferred to 35 °C water bath and stirred for 30 min. Then, 46 ml of deionized water was added and temperature of mixture was raised to 95 °C. The solution was stirred for another 20 min. After this, 6 ml H_2O_2 (30 wt.%) was added dropwise which resulted in change of the color of solution from dark brown to bright yellow. The synthetic mixture was repeatedly washed and centrifugalized with deionized water until the pH of solution was close to 7. Graphite oxide (GO) was obtained after drying at 60 °C under vacuum. Graphite oxide powder was dispersed in deionized water to create 1 mg/ml of dispersion, the color of which turned brown after ultra-sonication for 3 h.

2.1.2. Synthesis of graphene

Graphene was synthesized via chemical reduction of GO by using hydrazine hydrate as a reducing agent. For this purpose, 1 ml hydrazine hydrate was added into 100 ml graphite GO dispersion and the solution was heated in water bath to 80 °C for 24 h. Graphene gradually precipitated out as a black solid, which was filtered and washed repeatedly with deionized water. The synthesized graphene was stored in a desiccator.

2.2. Preparation of Ni-graphene composite coating

AISI 45 steel disks with φ43 mm and 4 mm thickness were used as substrate for deposition of coatings. The steel plates were mechanically polished with 180#, 320#, 400#, 600#, and 800# emery paper to get a smooth, bright and uniform surface, and then degreased in acetone and immersed in 10% HCl to remove dust and rust.

Composite coatings were prepared by multi-group reversing pulse electrodeposition method keeping pure Ni plate as anode and 45 steel disk as cathode. The Watt's electroplating bath used for the coating and the suspension was continuously stirred at a constant speed. The bath composition and operating conditions are given in Table 1. Prior to composite coating, the bath solution was stirred using a magnetic stirrer at 700 rpm for about 2 h, and subsequently by ultrasonic agitation for 1 h. After electrodeposition, the composite coatings were washed dried and then used for further studies.

2.3. Characterization of coatings

The hardness of composite coatings was estimated by Vickers hardness tester using a load of 200 g ($HV_{0.2}$). The surface and cross-section morphology of composite coatings were observed under scanning electron microscope (SEM). The phase and composition were analyzed by X-ray diffraction (XRD) using a Cu Kα radiation and Energy Dispersive Spectroscopy (EDS).

2.4. Tribological behavior testing

Dry sliding friction and wear tests were carried out using a WTH-2E ball-on-disk tribometer under the normal loads ranging from 1 to 3 N and a constant velocity of 0.1 m s^{-1}. A 4 mm diameter Si_3N_4 ceramic ball was used as the counterface against the AISI 45 steel discs coated with Ni-graphene composite coatings. The pure Ni coating was used for comparison. The wear rate was calculated in

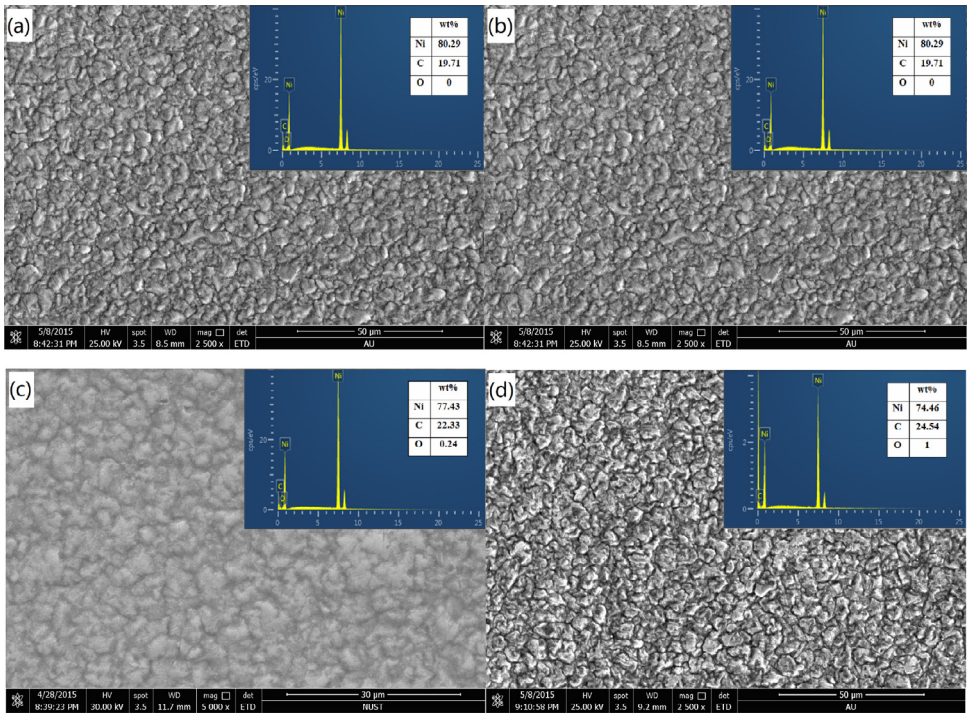

Fig. 5. SEM photomicrographs of Ni-graphene composite coatings with different amounts of graphene: (a) 0.1 g/L; (2) 0.2 g/L; (3) 0.3 g/L; (4) 0.4 g/L.

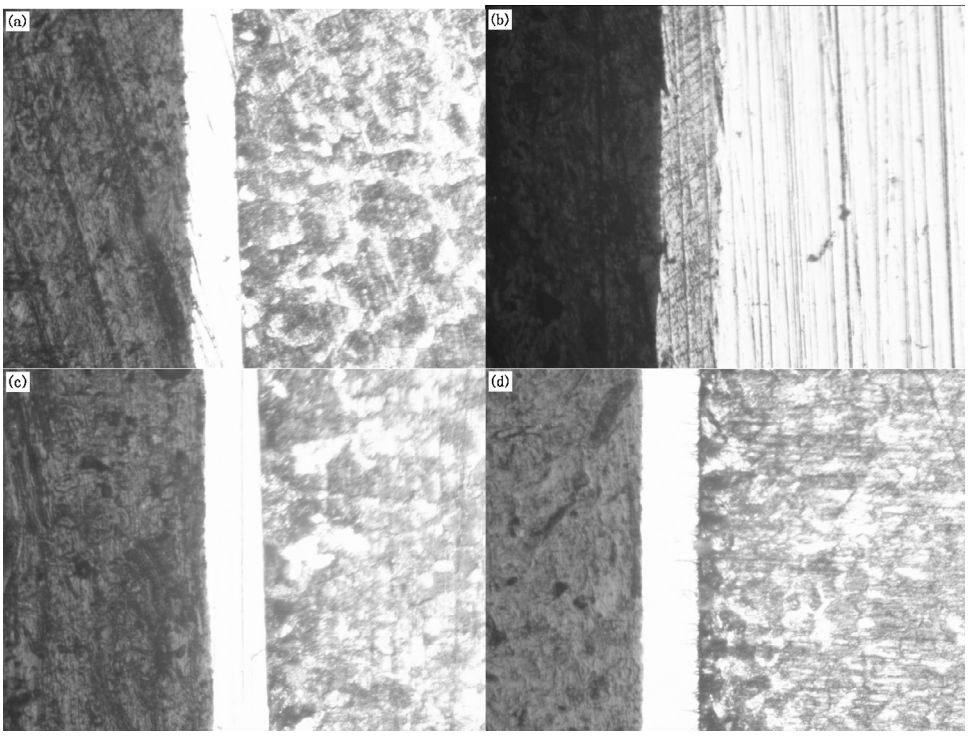

Fig. 6. Cross-sectional morphologies of composite coating: (a) 0.1 g/L; (b) 0.2 g/L; (c) 0.3 g/L; (d) 0.4 g/L.

terms of the mass loss measured by an analytical balance with a resolution of 0.0001 g.

3. Results and discussion

3.1. Characterization of graphene

Fig. 1 shows the XRD pattern of graphene reflecting the nanocrystalline nature of graphene and a broad peak at $2\theta = 24.7^{\circ}$, indicating the removal of oxygen-containing functional groups present in the interlayer spacing of the graphite oxide due to reduction process [10,11].

Raman spectra of pf both graphite oxide and graphene are shown in Fig. 2. Two strong peaks at 1354 cm^{-1} and 1594 cm^{-1}, referring to D and G mode, respectively, could be seen in the spectra. The ratio of ID and IG, i.e., ID/IG which is used as a measurement of the relative degree of disorder in carbonaceous materials [12], is found to be as 1.02 for graphene and 0.88 for graphite oxide. Fig. 3 depicts SEM photomicrographs of reduced graphite oxide showing stacked layer structure.

3.2. Characterization of Ni-graphene composite coating

3.2.1. XRD analysis

Fig. 4a shows the XRD patterns of composite coatings with different additions of graphene whereas, the patterns obtained for different bath temperatures and with a fixed addition of 0.1 g/L graphene are presented in Fig. 4b. One can see from Fig. 4a that, the intensity of peak increases gradually with increasing amount of graphene. However, at a fixed addition of graphene the intensity is observed to be maximum for a bath temperature of 60 °C, beyond which the intensity of peak decreases with increasing temperature. The average crystallite size of the deposits can be calculated from the Debye Sherrer's equation (1) [13].

$$L = \left(\frac{K\lambda}{\beta \cos\theta}\right) \quad (1)$$

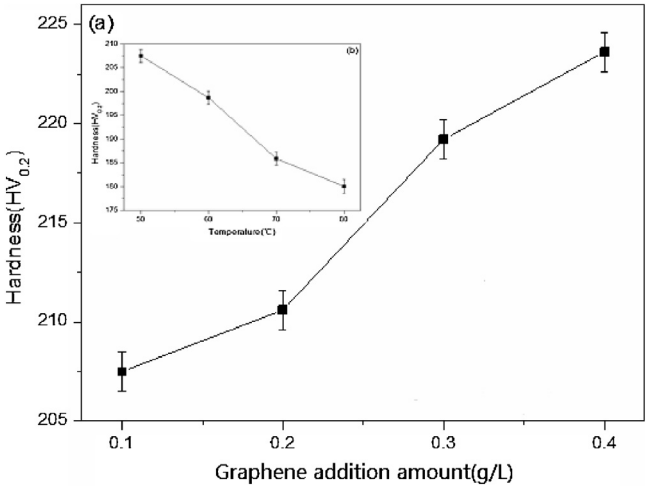

Fig. 7. Variation of micro-hardness of Ni-graphene composite coating with amount of graphene (a), bath temperature (b).

where L is the average crystallite size, K is the Scherer constant, λ is the wave length (0.154056 nm), β is the full width half maxima (FWHM), and θ is the diffraction angle. The average crystallite size decreases from 38.1 nm (0.1 g/L), 34.1 nm (0.2 g/L), 32.5 nm (0.3 g/L) to 31.0 nm (0.4 g/L) after calculation. Hence, one may conclude that the average crystallite size decreases with increasing amount of graphene. This may be explained on the basis of the fact that during the composite electrodeposition, the graphene enhances nucleation by creating a disorder in the matrix and simultaneously diffusion of graphene toward growing centers also helps in retardation of crystal growth, these mechanisms of increase in the nucleation growth and retardation in the crystal growth of composite brings about a reduction in the crystallite size [8]. These small sized particles may be the reason for the presence of strong diffraction peak which becomes even more prominent with the

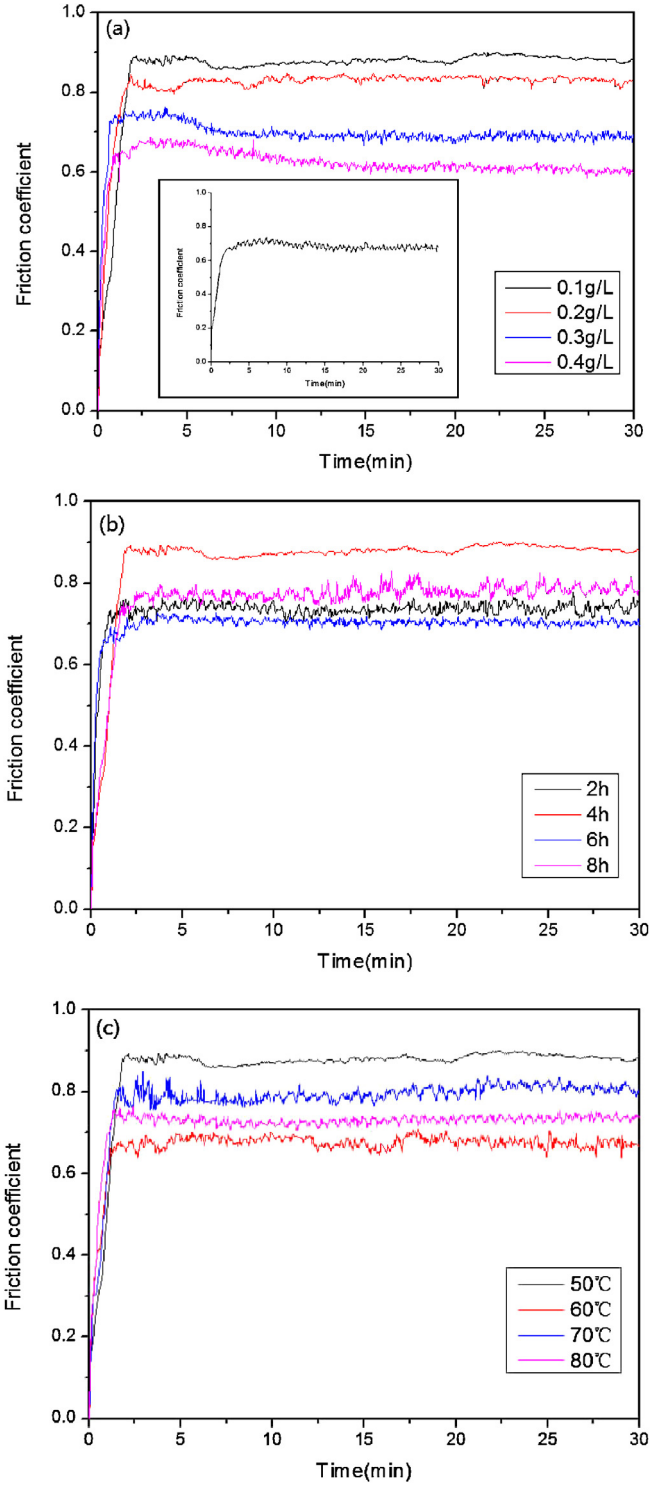

Fig. 8. Friction coefficient of composite coatings with different addition amount of graphene (a) and under different plating time (b) and different bath temperature (c) with 0.1 g/L graphene.

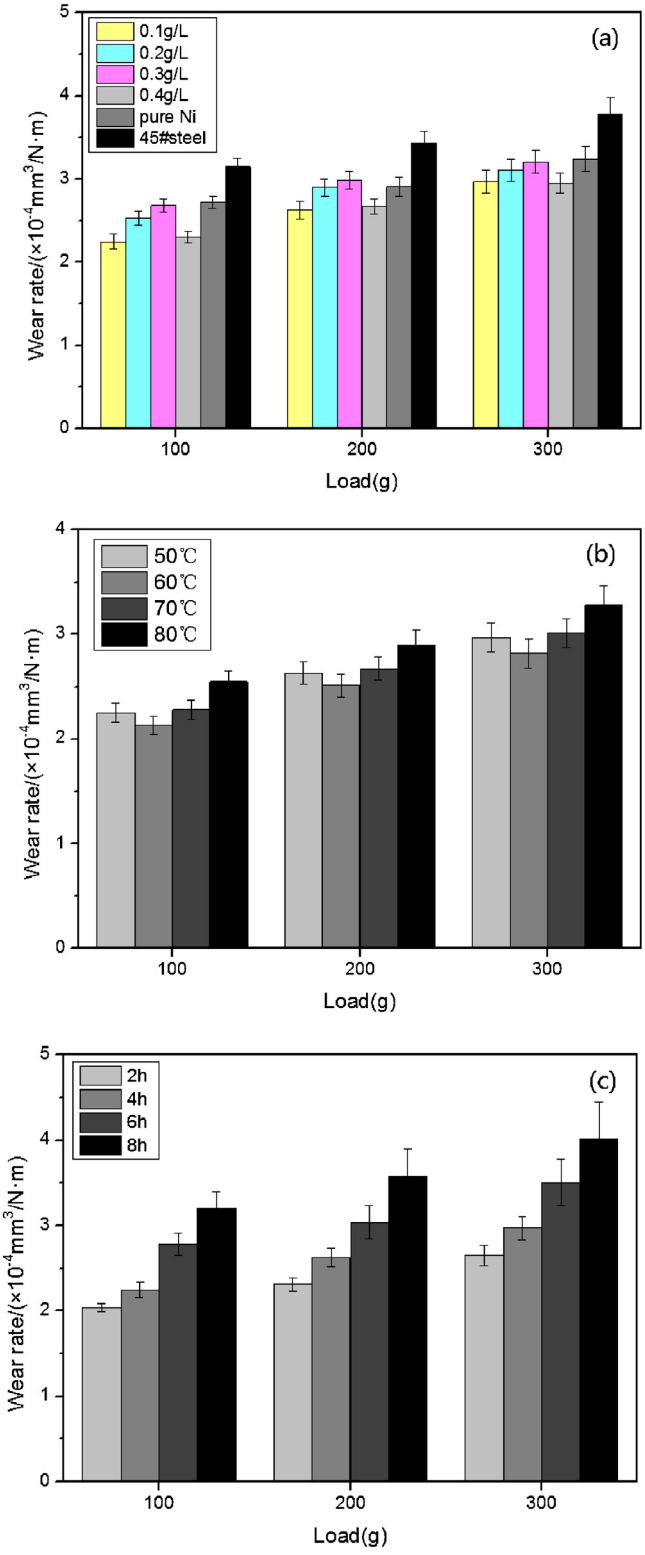

Fig. 9. Variation of wear rate of composite coatings (a) with different addition amount of graphene, (b) with different plating time, (c) under different plating time.

increasing amount of graphene. However, we could not detect the diffraction peak of graphene, probably due to the limitations of XRD as the amount of graphene may have been below the detection limit. The difference in the ID/IG ratio for graphene and GO may also be attributed due to the decrease in the average size of crystalline graphitic domains and formation of some smaller sp2 domains during reduction.

3.2.2. *SEM and EDS analysis*

Surface morphologies of Ni-graphene composite coatings are shown in Fig. 5. The composite coating depicts uniform structure with bright and small sized grains with increasing amount of graphene. The EDS analyses indicate that graphene adsorbed on the

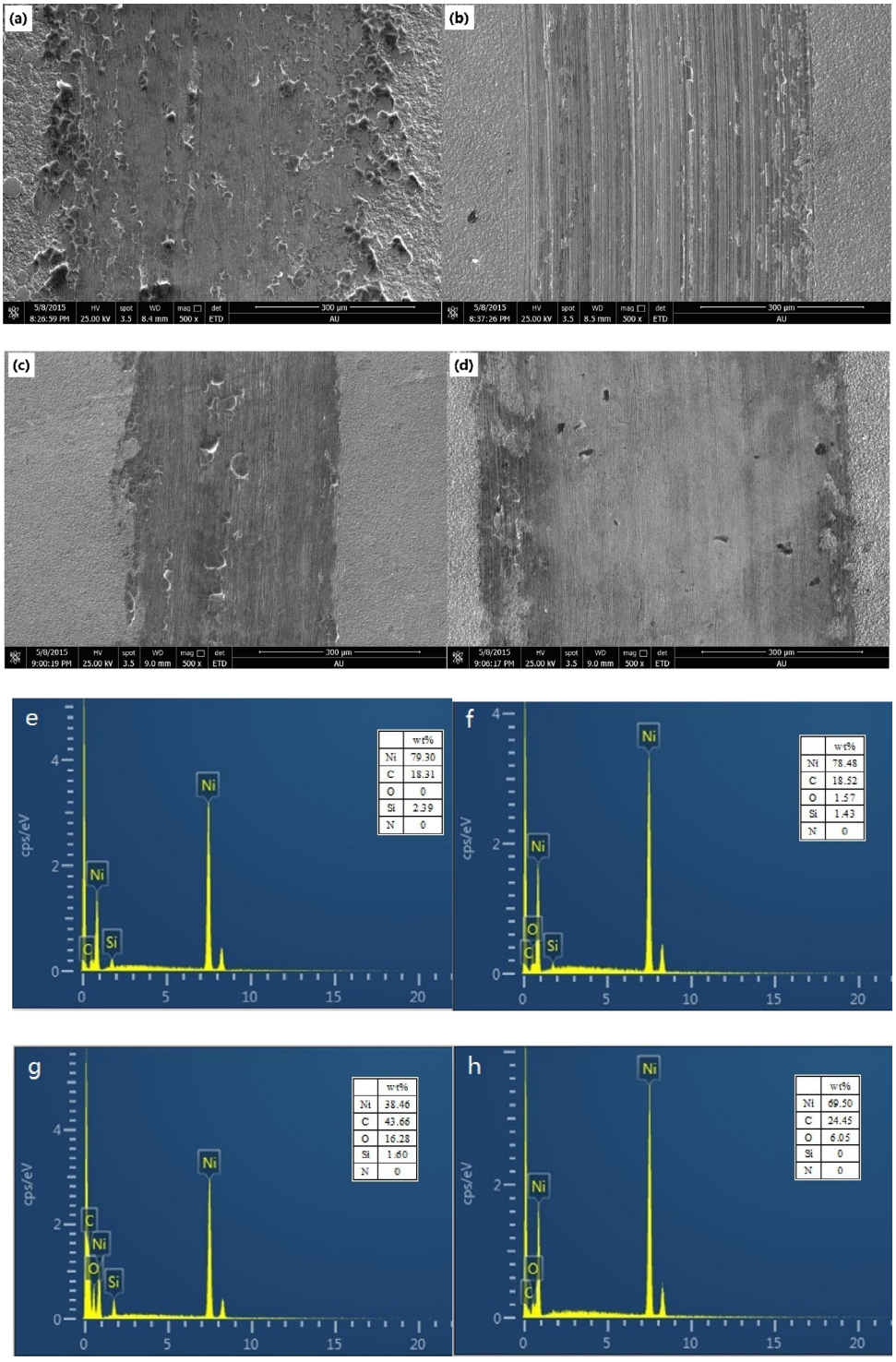

Fig. 10. SEM morphologies and EDS analyses of wear track: (a, e) 0.1 g/L; (b, f) 0.2 g/L; (c, g) 0.3 g/L; (d, h) 0.4 g/L.

plating surface during deposition hinders the crystal growth and increases the number of nucleation sites for reduction of Ni ions, resulting in a fine grained and intact arrangement of Ni crystals in the composite coating [14]. When graphene content is 0.3 g/L or more, a small amount of O is detected probably due to the oxidation of C in the coating.

3.2.3. Cross-sectional morphologies of composite coating

Fig. 6 (a through d) shows cross-sectional morphologies of composite coating with 0.1 g/L and 0.4 g/L graphene addition, respectively, as observed under metallographic microscope. A comparison of Fig. 6a–d of graphene shows that the average thickness of coating increases with increasing amount of graphene. The coating thicknesses for the additions of 0.1, 0.2, 0.3 and 0.4 g/L are 73.5, 78.6, 85.1 and 89.5 μm, respectively. Further, one could also observe that the coating is well bonded to the substrate with no obvious defects and impurities visible at the interface. It may be attributed to the absorption of graphene particles on the substrate resulting in a firm bonding between the coating and the substrate.

3.2.4. The Vickers micro-hardness

Fig. 7a shows the variation of Vickers micro-hardness of Ni-graphene composite coatings with graphene content. Fig. 7b depicts the variation of hardness with the bath temperature for a fixed amount of graphene addition of 0.1 g/L and fixed time of coating of 4 h. It can be seen that the Vickers micro-hardness ($HV_{0.2}$) of composite coating increases with increasing amount of graphene. However, the hardness decreased with increasing both the bath temperature for a fixed addition of 0.1 g/L as evident from Fig. 7b. The increase in hardness with increasing amount graphene can be explained on the basis of the finer grain size which is observed in the present study which provides hindrance to the movement of dislocations resulting in improved resistance to plastic flow and enhanced hardness. At the same time, the inherent high mechanical strength of graphene might also have played a vital role in improving the hardness of the composite coating [15]. However, the movement of dislocations might have become easier with the increase in bath temperature during plating, leading to the lower hardness of the coating.

3.3. Friction and wear behavior

The variation of friction coefficient of composite coatings with different amounts of graphene tested at a normal load of 2 N against the ball of Si_3N_4 is illustrated in Fig. 8a while the variations of friction coefficient with bath temperature and plating time for a fixed addition of 0.1 g/L graphene under the same testing conditions are shown in Fig. 8b and c, respectively. One can observe that the friction coefficient sharply increases to a certain value, stabilizes and then maintains a constant magnitude during the whole test and the trend is similar for all the coatings containing different additions of graphene as evident from Fig. 8a. However, the friction coefficient is found to decrease with increasing amount of graphene and the value reaches to 0.6 for the coating containing the highest amount of graphene i.e., 0.4 g/L, used in the present work. The friction coefficient of pure Ni coating is observed to be about 0.7 as shown in the inset in Fig. 8a. The friction coefficients shown by the coatings having 0.1 g/L and 0.2 g/L graphene are a little bit higher than 0.7 whereas the friction coefficient of the coating having 0.3 g/L graphene is nearly same as that of pure Ni coating as evident from Fig. 8a. Thus one may conclude that the addition of graphene should be more than 0.3 g/L for being effective in reducing the friction, which is also commensurate with the Raman analysis. Gomez-Navarro et al. [16], Poot et al. [17], and Frank et al. [18] studied the mechanical properties of graphene and reported the high young's modulus of graphene hinders the formation of a lubricating film of graphene when the amount of graphene is less. So, the friction coefficient does not decrease but increase compared with the pure Ni, probably because of high mechanical strength of graphene itself. When graphene content is more than 0.3 g/L, the reduction in friction coefficient occurs by forming a layer of lubrication film. With the rise of bath temperature, the friction coefficient first decreases and then increases. In the present study, the lowest value of friction coefficient (about 0.68) is obtained at a bath temperature of 60 °C. The friction coefficient does not show any consistent trend of variation with time of plating, but it shows the lowest value of 0.7 for a plating time of 6 h. Therefore, one may conclude that a bath temperature of 60 °C and plating time of 6 h are the best experimental parameters as far as frictional behavior is concerned.

3.3.1. Wear rate

In order to further evaluate the wear resistance and adhesion of coatings, wear rate has been used to clarify the tribological properties. Fig. 9 presents the variation of wear rate composite coatings with different addition amount of graphene, under different plating temperature and with different plating time with different load at 0.1 m s^{-1} after sliding for 30 min. It can be seen in Fig. 9a that under the same load, wear rate increases with the increase of addition amount of graphene. Similarly, wear rate of composite coatings increases with the increase of load under the same addition amount of graphene. The wear rate of 45 steel is the largest. When the amount of graphene increases from 0.3 g/L to 0.4 g/L, the wear rate starts to decrease, which is probably associated with the compact structure (see Fig. 5d) and the high hardness of coatings (see Fig. 7), giving rise to an improvement of the load bearing capacity and the wear resistance. As is shown in Fig. 9b, when the plating temperature is 60 °C, the value of wear rate is the lowest at all the load. Then it rises along with the temperature rise. Prolong the deposition time may help in thickening composite coatings, but the coatings have shown a limited improvement in wear resistance as shown in Fig. 9c. This may be attributed to a relatively lower hardness (Fig. 7b), resulting in a reduced load bearing capacity.

3.3.2. SEM and EDS analyses of wear track

Fig. 10 shows SEM morphologies and EDS analyses of wear track with different amount of graphene. In contrast to the coated surface, regular surface helps in improving its resistance to penetration against Si_3N_4 ball and leads to a regular wear track as shown in Fig. 3b. In comparison to Fig. 8a, loose structure and low hardness may be the reasons why the wear track appears irregular. One can also see some layers ready to get off (Fig. 10c). The wear track in Fig. 10d is mild and flat, which is attributed to the compact surface (Fig. 5d) and the high hardness (Fig. 7). EDS analysis (Fig. 10g) displays that there exist more O and C content, and oxidation during the tribo-testing may be the probable reason for the peeling of the layer. All the coatings exhibit relatively serious wear in dry sliding conditions but without wear through, indicating that coatings adhere well with the steel substrate. It is believed that the wear of Si_3N_4 ball might have occurred which leading to the transfer of material from the ball to the counterface as depicted in EDS analyses in Fig. 10e to 10 g.

4. Conclusions

In the present work, graphene was synthesized from graphite oxide and characterized. The Ni-graphene coating was successfully coated on the steel specimen. The presence of graphene in the deposited coating was confirmed by EDS analyses and Raman spectra. The presence of graphene made the surface morphology of composite coating more compact, and the hardness became higher with the increase of addition amount of graphene. All the results revealed that the optimum experimental parameters were 60 °C of bath temperature and 6 h of plating time. Besides, less amount of graphene does not seem to lead to the remarkable reduction of friction coefficient compared with pure nickel coating, however, the value starts to decrease when the addition amount increases to 0.4 g/L. Hence, the higher addition amount of graphene is helpful for reducing friction coefficient of composite coatings.

Acknowledgements

This project is supported by National Natural Science Foundation of China (No. 51101087), Natural Science Foundation of Jiangsu Province (No. BK20151487), China Postdoctoral Science Foundation (Nos. 2013M540450, 2014T70520) Fundamental Research Funds for the Central Universities (No. 30915014103) and a project funded by the Priority Academic Program Development of Jiangsu Higher Education Institutions and the Zijin Intelligent Program, Nanjing University of Science and Technology.

References

[1] E. Garcia-Lecina, I. Garcia-Urrutia, J.A. Diez, M. Salvo, F. Smeacetto, G. Gautier, R. Seddon, R. Martin, Electrochim. Acta 54 (2009) 2556.
[2] C.M. Praveen Kumar, T.V. Venkatesha, K.G. Chandrappa, Surf. Coat. Technol. 206 (2012) 2249–2257.
[3] L. Chen, L. Wang, Z.X. Zeng, J. Zhang, Mater. Sci. Eng. A 434 (2006) 319–325.
[4] X.Z. He, Y.X. Wang, X. Sun, L.Y. Huang, Prep. Nanosci. Nanotechnol. Lett. 4 (2012) 48.
[5] C.R. Carpenter, P.H. Shipway, Y. Zhu, Wear 271 (2011) 2100–2105.
[6] K.S. Novoselov, A.K. Geim, S.V. Morozov, D. Jiang, Y. Zhang, S.V. Dubonos, I.V. Grigorieva, A.A. Firsov, Science 306 (2004) 666–669.
[7] K.S. Kim, H.J. Lee, C. Lee, S.K. Lee, H. Jang, J.H. Ahn, J.H. Kim, ACS Nano 5 (2011) 5107–5114.
[8] C.M. Praveen Kumar, T.V. Venkatesha, R. Shabadi, Mater. Res. Bull. 48 (2013) 1477–1483.
[9] W.S. Hummers, R.E. Offeman, J. Am. Chem. Soc. 80 (1958) 1339.
[10] Z. Lei, L. Lu, X.S. Zhao, Energy Environ. Sci. 5 (2012) 6391–6399.
[11] S. Park, J. An, J.R. Potts, A. Velamakanni, S. Murali, R.S. Ruoff, Carbon 4 (2011) 3019–3023.
[12] S. Yang, W.B. Yue, D.Z. Huang, C.F. Chen, H. Lin, X.J. Yang, RSC Adv. 2 (2012) 8827–8832.
[13] S. Ramalingam, V.S. Murulidharan, A. Subramania, J. Solid State Electrochem. 13 (2009) 1777–1783.
[14] B.M. Praveen, T.V. Venkatesha, Appl. Surf. Sci. 254 (2008) 2418–2424.
[15] B.M. Praveen, T.V. Venkatesha, J. Alloys Compd. 482 (2009) 53–57.
[16] C. Gomez-Navarro, M. Burgard, K. Ken, Nano Lett. 8 (2008) 2045–2049.
[17] M. Poot, H.S.J. van der Zant, Appl. Phys. Lett. 92 (2008) 063111.
[18] I.W. Frank, P.M. Tanenbaum, A.M. van der Zande, J. Vac. Sci. Technol. B 25 (2007) 2558–2561.